

Journal of Materials Chemistry C

Accepted Manuscript



This is an *Accepted Manuscript*, which has been through the Royal Society of Chemistry peer review process and has been accepted for publication.

Accepted Manuscripts are published online shortly after acceptance, before technical editing, formatting and proof reading. Using this free service, authors can make their results available to the community, in citable form, before we publish the edited article. We will replace this *Accepted Manuscript* with the edited and formatted *Advance Article* as soon as it is available.

You can find more information about *Accepted Manuscripts* in the [Information for Authors](#).

Please note that technical editing may introduce minor changes to the text and/or graphics, which may alter content. The journal's standard [Terms & Conditions](#) and the [Ethical guidelines](#) still apply. In no event shall the Royal Society of Chemistry be held responsible for any errors or omissions in this *Accepted Manuscript* or any consequences arising from the use of any information it contains.

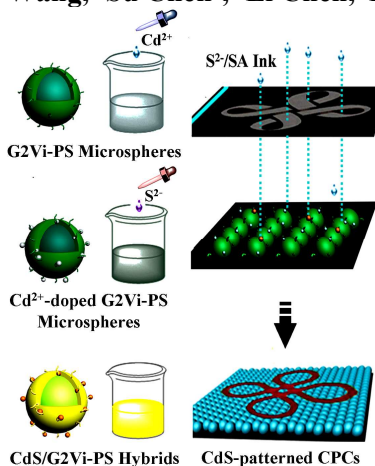
Cite this: DOI: 10.1039/c0xx00000x

www.rsc.org/xxxxxx

ARTICLE TYPE

Versatile Dendrimer-Derived Nanocrystal Microreactors towards Fluorescence Colloidal Photonic Crystals

¹Jing Zhang, ¹Luting Ling, ¹Cai-Feng Wang, ¹Su Chen*, ¹Li Chen, ²David Y. Son



⁵ Versatile dendrimer-derived nanocrystal microreactors were first demonstrated in this work to fabricate self-assembled functional colloids and photonic materials.

Cite this: DOI: 10.1039/c0xx00000x

www.rsc.org/xxxxxx

ARTICLE TYPE

Versatile Dendrimer-Derived Nanocrystal Microreactors towards Fluorescence Colloidal Photonic Crystals

¹Jing Zhang, ¹Luting Ling, ¹Cai-Feng Wang, ¹Su Chen*, ¹Li Chen, ²David Y. Son

Received (in XXX, XXX) Xth XXXXXXXXX 200X, Accepted Xth XXXXXXXXX 200X

DOI: 10.1039/b000000x

The ability to finely bind colloidal photonic crystals with nanocrystals (NCs) is critical in many applications ranging from light-emitting devices to flexible displays and biological labels. Herein, the use of the carbosilane-thioether generation 2 vinyl-terminated (G2-Vi) dendrimers facilitates the zero dimensional (0D) and two dimensional (2D) microreactors with high uptaking NCs, allowing them to generate fluorescent colloidal photonic crystals. Dendrimer-functionalized microspheres were prepared by seeded copolymerization from micrometer-sized polystyrene (PS) seed particles and G2-Vi dendrimers. As an independent 0D microreactor, such dendrimer-functionalized microsphere lattices bearing abundant thioether anchor sites can capture guest metal ion components, followed by the introduction of chalcogenides, and hence the *in situ* generation of higher-uptake NCs was realized. Furthermore, the as-obtained NC-latex hybrids from 0D microreactors were directly self-assembled into large-scale ordered colloidal arrays with uniform fluorescence. Additionally, compact assemblies from the Cd²⁺-loaded dendrimer-functionalized microspheres were constructed and were employed as a large-scale 2D reactor. An on-demand fluorescence pattern was freely and quickly displayed via reaction-induce-response process by screen stencil oriented printing.

Introduction

Colloidal photonic crystals (CPCs), with characteristic of photonic band-gap, have stimulated great interest due to their unique light manipulation and inhibition capability.¹⁻¹⁵ Recently, the incorporation of various nanocrystals (NCs) into CPCs is of special interest, because not only high refractive index contrast of CPCs towards a full photonic bandgap is expected but also great enhancement of the fluorescence properties of incorporated NCs is achieved through resonance with the periodic structures. Tremendous methods, such as physically entrapment,¹⁶⁻¹⁸ controlled heterocoagulation,^{19,20} and LbL deposition,²¹⁻²⁴ have been proposed for preparing the NC/CPC hybrids with applications in areas ranging from light-emitting devices to flexible displays and biological labels. Despite great advances in this field, much work is still highly needed. For instance, the incorporation of preformed NCs onto CPCs are often accompanied with the agglomeration of the NCs, which leads to the fluorescence diminishing or the quenching of the NCs and restricts the corresponding practical applications.

Recently, the use of defined polymers as nano- or micro-reactors for NC synthesis provides a valuable insight to the

preparation of NC/polymer hybrids without mentioned drawbacks. Since Antonietti's group first proposed the use of microgels as nanoreactors for NC synthesis,²⁵ polymer-based nano- or micro-reactors have been employed effectively to prepare plenty of materials with structural hierarchy.²⁶⁻³³ Whereas, the process to incorporate various NCs into these reactors normally leads to irregular morphologies and low surface charges, which will impose negative effects on following steps for CPC assembly. Thus, an alternative method to synthesize well-defined NC-colloidal particles is still highly desired. Additionally, the further exploration of in-situ NC synthesis within ordered colloid array, which is rarely involved in previous study, is also critical to LED, encoding, anti-counterfeit and a set of relevant applications.³⁴⁻³⁹

In this work, we demonstrated a new avenue to fluorescent CPCs with high uptaking NC by using dendrimer-derived zero-dimensional (0D) and two-dimensional (2D) microreactors for the first time. The dendrimer-functionalized microspheres were obtained by seeded copolymerization of micrometer-sized polystyrene (PS) microspheres with the carbosilane-thioether generation 2 vinyl-terminated (G2-Vi) dendrimers. As an independent 0D microreactor, dendrimer-functionalized microspheres bearing abundant thioether anchor sites can efficiently capture guest metal ion components, and hence the *in situ* generation of higher-uptake NCs was realized by introduction of metal ions and subsequent chalcogenides into the lattices. Moreover, the as-obtained NC-latex hybrids from the 0D microreactor were directly self-assembled into large-scale ordered colloidal arrays, providing advantages for growth of

¹State Key Laboratory of Material-Oriented Chemical Engineering, College of Chemistry and Chemical Engineering, Nanjing University of Technology, 5 Xin Mofan Road, Nanjing 210009, P. R. China. ²Southern Methodist University, Chemistry, Dallas, Texas, United States. E-mail: chensu@njut.edu.cn; Fax: 86-25-83582258; Tel: 86-25-83172258; † Electronic supplementary information (ESI) available: Experimental details and additional characterization data. See DOI: 10.1039/b000000x

high-quality CPCs with uniform and stable fluorescence. Additionally, compact assemblies from the Cd²⁺-loaded dendrimer-functionalized microspheres were prepared and employed as a large-scale 2D microreactor. By using a screen stencil oriented printing technique, an on-demand fluorescent pattern was freely and quickly displayed via a reaction-induce-response process, suggesting an alternative way to selectively and effectively construct NC-integrated CPCs. The fundamental knowledge gained from the study of these 0D and 2D NC microreactors will facilitate progress in the field of self-assembled functional colloids and photonic materials.

Experimental

Materials

Styrene (St) was purified by distillation under reduced vacuum to remove inhibitor. Potassium persulfate (KPS), cadmium chloride (CdCl₂•2.5H₂O), thioglycolic acid (TGA), sodium sulfide (Na₂S•9H₂O), sodium hydroxide (NaOH), divinylbenzene (DVB), ethanol (C₂H₅OH) and polyvinylpyrrolidone (PVP) were of analytical grade and used as received. Purified water with resistance greater than 18 MΩ cm was used in all experiments. The dendrimers, carbosilane-thioether generation 2 vinyl-terminated (G2-Vi) dendrimer, were synthesized by previously reported methods.⁴⁰

Preparation of dendrimer-functionalized polystyrene microspheres.

The synthesis of G2-Vi dendrimer-functionalized polystyrene microspheres used as the 0D nanocrystal (NC) microreactor in this work was achieved by seeded copolymerization from micrometer-sized PS seed microspheres and G2-Vi dendrimers. Briefly, 130 mL of deionized water was poured into a four-necked, round-bottomed flask equipped with a condenser, a nitrogen inlet, a thermometer and a stirrer. Then 6.50 g of purified styrene, 0.10 g of DVB, 0.24 g of PVP and 0.04 g of KPS were added with stirring under a N₂ gas atmosphere. The reaction was initiated by increasing the temperature to 98 °C. After the reaction was kept at 98 °C for 2 h under constant stirring, 0.5 g of styrene, 0.015 g of DVB, 0.75 g of G2-Vi dendrimers and 0.008 g of KPS in 15 mL of deionized water were added dropwise slowly, and the reaction was terminated after about 4 h to give the final G2Vi dendrimer-functionalized polystyrene microspheres. The resulting particles serving as the 0D NC microreactor were finally obtained after purified with a 200-mesh nylon net to remove minor traces of agglomerates.

In situ synthesis of CdS NCs in the 0D microreactor.

The *in situ* synthesis CdS NCs within the 0D microreactor were carried out as follows: First, under vigorous stirring, 0.5 g of dendrimer-functionalized microspheres were dispersed into a solution containing 0.228 g (1 mmol) CdCl₂•2.5H₂O, 0.185 g (2 mmol) TGA in 30 mL of deionized water. The pH value of the mixture was adjusted to neutral by aqueous solution of NaOH (1 M). Subsequently, the resulting Cd²⁺-loaded dendrimer-functionalized microspheres were purified by centrifugation at 12 000 rpm and then redispersed in 30 mL of deionized water. Finally, 0.015g (0.06 mmol) of Na₂S•9H₂O dissolved in 5 mL of deionized water were added, and the reaction was terminated

after about 2 h to give the final CdS-latex hybrids. The as-obtained products were further purified by centrifugation to remove minor CdS NCs which were weakly attached on the surface of the products and dried at room temperature under vacuum.

TGA-stabilized CdS NCs serving as the control sample were also synthesized here using a sol-gel method.^{41,42} First, 0.228 g (1 mmol) of CdCl₂•2.5H₂O was dissolved in 25 mL deionized water. Then 0.185 g (2 mmol) TGA dissolved in 5 mL deionized water was added into the above solution under vigorous stirring, followed by adjusting the pH value to neutral via dropwise addition of 1 M NaOH solution. Subsequently, 0.240 g (1 mmol) of Na₂S•9H₂O dissolved in 5 mL of deionized water were added to give the CdS NCs. The final samples were further purified by adding absolute ethanol and then centrifuged at 5 000 rpm.

Construction of colloidal photonic crystals (CPCs)

A modified inward-growing self-assembly method was adopted here for quick fabrication of the CPC films.⁴³ A colloidal suspension with concentration of 2 wt% was dropped on the glass substrate and spread to cover the substrate which was prior treated with a chromic-sulfuric solution for 12 h. Subsequently, move the substrate to the oven to complete crystallization at 25 °C with a relative humidity of 70 %. The fluorescent CPC film with bright structure colour was finally obtained after evaporation of solvents.

Construction of CdS-patterned CPCs via a reaction-induce-response process

The 2D CPC-based reactor used as the substrate for silk-screen printing was constructed from compact assemblies of the Cd²⁺-loaded dendrimer-functionalized microspheres via a vertical deposition method. Detailed procedures were depicted as follows.⁴⁴ Glass slides used to perform the assembly were first cleaned by a chromic-sulfuric acid solution. To initiate the assembly process, the treated glass substrate were vertically immersed into colloidal suspensions of the Cd²⁺-loaded dendrimer-functionalized microspheres of 0.2 wt% at a constant temperature of 80 °C and a relative humidity of 60 %. Following the evaporation of water, the 2D CPC-based reactor was fabricated.

The preparation of CdS-patterned CPCs was achieved by the aid of silk screen printing with the use of the as-obtained 2D CPC-based reactor as the printing substrate. Firstly, the printing “ink” containing Na₂S was prepared by mixing the Na₂S aqueous solution with a certain amount of sodium alginate (SA). Then, quickly cast the ink onto the printing mask, and penetrate the ink through the “Chinese Knot” pattern screen (160 meshes) onto the 2D CPC-based reactor below. Via the reaction-induce-response process, fluorescent patterns emerged on the substrate, resulting in the formation of CdS-patterned CPCs.

Characterization.

Fourier transform infrared (FT-IR) spectra were recorded on a Nicolet 6700 FT-IR spectrometer. Scanning electron microscope (SEM) observations were obtained using a HITACHI S-4800 scanning electron microscope. Energy-dispersive Spectrum (EDS) measurements were performed with the energy-dispersive X-ray spectrometer attached on the S-4800 SEM. The

X-ray diffraction (XRD) patterns were conducted on a Bruker-AXS D8 ADVANCE X-ray diffractometer with Cu-K α radiation ($\lambda=0.1542$ nm) at a scanning speed of 6 $^{\circ}$ /min over 2θ range of 10-80 $^{\circ}$. The microstructures of as-prepared CdS/G2Vi-PS hybrids were examined by using a transmission electron microscope (TEM) (JEOL JEM-2100). The sample was placed on a copper grid, which was left to dry before being transferred into the TEM sample chamber. Fluorescence spectra were recorded on a Varian Cary Eclipse spectrofluorometer with 370 nm laser beam as a light source. Ultraviolet-visible (UV-vis) spectra and reflectance spectra were obtained on an optical microscope equipped with a fibre optic spectrometer (Ocean Optics, USB 4000). Photoluminescence (PL) measurements were carried out on a Varian Cary Eclipse spectrophotometer and the quantum yield was calculated by comparison using quinine sulfate in 0.10 M H $_2$ SO $_4$ solution as the standard ($\Phi = 0.54$). Photographs were taken with an optical microscope (ZEISS, Axio Scope.A1).

Results and Discussion

The synthesis of dendrimer-functionalized polystyrene (G2Vi-PS) microspheres which serve as an independent 0D microreactor is achieved by seeded copolymerization of micrometer-sized PS microspheres with the carbosilane-thioether generation 2 vinyl-terminated (G2-Vi) dendrimers. As shown in Fig. 1a, the well-defined dendrimers selected here are composed of terminal double bond groups and abundant thioether groups in the interior. These features allow them to copolymerize with the PS seed microspheres via free radical polymerization, and to form the 0D microreactor with plenty of thioether anchors for guest metallic precursors.^{40, 45-47} A typical SEM image of the as-synthesized microspheres is shown in Fig. 1b, from which we can see that they were highly monodispersed with a mean diameter of 226 nm. The character of uniform size ensured the microreactor potential to be further assembled to colloidal photonic crystals (CPCs).

To verify the successful incorporation of G2-Vi dendrimers, the exact surface components of the resulting microspheres were firstly examined by EDS. As shown in Fig. 1c, the elements including silicon and sulfur are facilely detected, demonstrating the successful incorporation of G2-Vi dendrimers. Besides, the facile detection of relevant elements here also presents the exposure of thioether groups on the surface of G2Vi-PS microspheres, which may favour a good contact between the dendrimer and the guest metallic precursors. In addition, the as-synthesized microspheres were also characterized by the FT-IR spectroscopy. Curves 1, 2, and 3 in Fig. 1d correspond to the FT-IR spectra of pure PS microspheres, G2-Vi dendrimers and the resulting G2Vi-PS microspheres, respectively. Upon comparing Curve 3 with Curve 1, a new absorption peak is noted at 1270 cm^{-1} , which are attributed to the stretching vibration peaks of the Si-CH $_2$ bond originated from the G2-Vi dendrimers (Curve 2). This result further confirms the successful synthesis of G2Vi-PS microspheres. The thermal stability of the as-obtained G2Vi-PS microspheres was determined by a thermogravimetric analyzer. As seen in Fig. 1e, the decomposition of PS seed microspheres occurs at 405-438 $^{\circ}$ C, while that of the G2Vi-PS microspheres undergoes at 412-443 $^{\circ}$ C. An enhanced thermal stability for the G2Vi-PS microspheres is attributed to the incorporation of

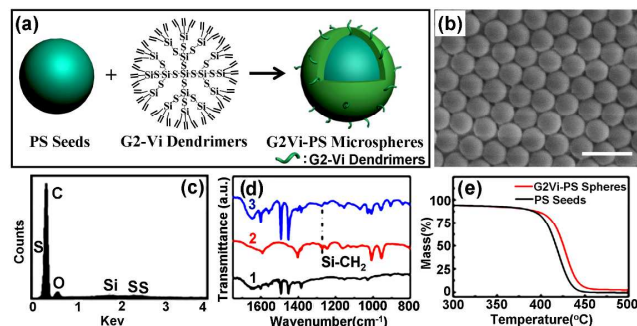


Fig. 1 (a) Scheme illustration of the preparation of the 0D microreactor. (b) SEM image of the as-obtained G2Vi-PS microspheres (Scale bar = 500 nm). (c) EDS spectrum of the as-synthesized 0D microreactor; (d) FT-IR spectra of PS seed microspheres (Curve 1), G2-Vi dendrimers (Curve 2) and the 0D microreactors (Curve 3), respectively. (e) Thermogravimetric curves of the PS seed microspheres and G2Vi-PS microspheres.

inorganic silica constituents originated from the G2-Vi dendrimers. The expected TGA weight residual, if the G2Vi-PS microspheres degraded to form SiO $_2$, is 3.2 %, compared with the experimentally observed weight residual of 2 %; thus, a graft efficiency of *ca.* 62.5% is obtained here.

Based on the above results, we can confirm the G2-Vi dendrimers have been successfully incorporated into PS microspheres, to afford dendrimer-functionalized microspheres, in which abundant thioether groups are exposed on the surface of the microspheres. These features enable the as-obtained G2Vi-PS microspheres to encapsulate and stabilize metallic components, and to behave ideal candidates as independent 0D reactors for NC synthesis.

The schematical illustration for synthesis of CdS NC in the 0D microreactor is shown in Fig. 2a. The G2Vi-PS microspheres were first immersed into the aqueous solution containing TGA/Cd $^{2+}$ complex. The Cd $^{2+}$ ions loading on microspheres can further react with sulfide source (Na $_2$ S solution) at room temperature, forming CdS NCs with yellowish-green fluorescence (inset of Fig. 2b). The resulting CdS-latex hybrids were characterized by XRD (Fig. 2b). Compared with the diffraction feature of the G2Vi-PS microspheres (Curve a), two

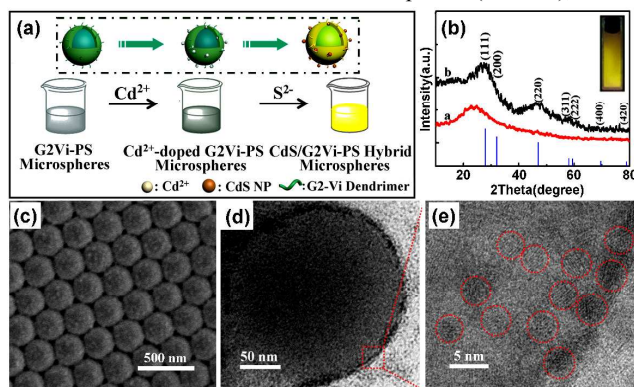


Fig. 2 (a) Scheme illustration of the preparation of CdS NCs in the 0D microreactor. (b) XRD patterns of G2Vi-PS particles (Curve a) and CdS/G2Vi-PS hybrid microspheres (Curve b). Inset: fluorescence image of the aqueous solution of CdS-latex hybrids. (c) SEM image of the as-obtained CdS-latex hybrids. TEM images of the CdS/G2Vi-PS hybrids at (d) low and (e) high magnification.

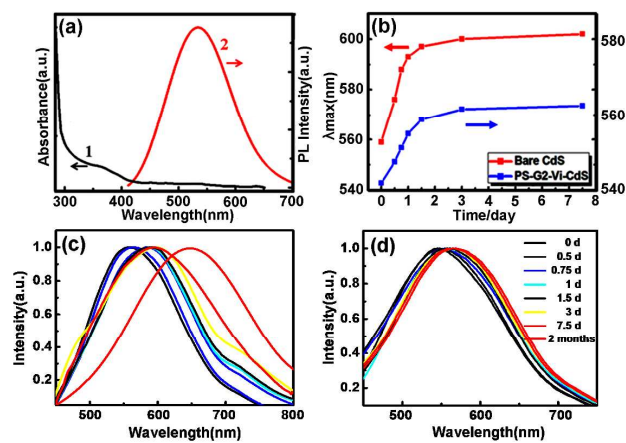


Fig. 3 (a) UV-vis absorption and PL spectra of CdS-latex hybrids. (b) the change in PL peak of the control sample (left) and as-obtained CdS-latex hybrids (right) as function of time. The detailed evolution process of the PL peak of the control sample (c) and CdS-latex hybrids (d).

new diffraction peaks of the as-synthesized CdS-latex hybrids (Curve b) appear at about 28.2° and 47.0° , corresponding to the (111) and (220) planes of cubic CdS (JPCSD 21-0829), respectively, suggesting the formation of cubic CdS NC in the 0D microreactor. Scanning electron microscopy (SEM) was also conducted here to visualize the morphology of as-obtained CdS-latex hybrids. As shown in Fig. 2c, the as-obtained CdS-latex hybrids are very regular, and the G2Vi-PS microspheres are uniformly surrounded by the as-prepared CdS NCs. The TEM image of the hybrid shown in Fig. 2d indicates that the shell layer of spherical domain (namely the G2Vi-PS microspheres) is densely surrounded by CdS NCs, presenting the high uptake of CdS NCs within the shell of G2Vi-PS microspheres. From the HRTEM image in Fig. 2e, the lattice fringes for a single CdS NC can be clearly distinguished. It can be seen that the as-obtained NCs are well dispersed without obvious aggregation due to existence of stabilizing ligand of dendrimers with abundant thioether groups.

The optical properties of the as-synthesized CdS NCs with the 0D reactor were investigated, as shown in Fig. 3a. A broad photoluminescent (PL) emission centred at 545 nm was observed when excited at 370 nm, indicating the formation of CdS NCs. The as-generated CdS NCs show UV-vis absorption at around 375 nm. According to the Brus's formula, the average size of CdS NCs is ca. 4 nm. The QYs of the control sample (TGA-stabilized CdS NCs) and as-obtained CdS-latex hybrids were also estimated here. The QY of as-obtained CdS-PS hybrids are improved from 2.5% (the control sample) to 4.8% (CdS-latex hybrids). It may be due to the prolonged assembly time for NC surface reconstruction and better passivation effect on the surfaces of as-synthesized CdS NCs within dendrimer-derived microreactors, thus resulting to improved PL performance.

Fig. 3b shows the change in PL peaks of the control sample and as-obtained CdS-latex hybrids in a week. The PL peak position of the control sample increases over time. Only when it reaches the red part of the spectrum, the growth velocity remarkably decrease. While quite different phenomena occur for the CdS-latex hybrids. Their PL peak position redshifts to longer wavelength at the beginning. However, 24 h later, it achieves the maximum value of 559 nm and no obvious change occurs

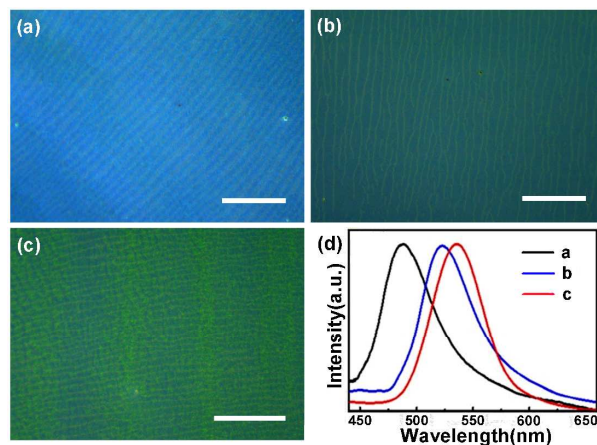


Fig. 4 Optical photographs of CPC films constructed by (a) PS seed microspheres, (b) G2Vi-PS microspheres and (c) CdS-latex hybrids, and (d) their corresponding reflection spectra. Scale bar: 200 μm .

afterwards, indicating that the as-prepared CdS NCs in this case have more stable fluorescence.⁴⁸ We ascribe these phenomena to the confinement effect of the microreactor. As the microreactor offers a polymer-surrounded environment, it makes the mass transfer process in/among the CdS-latex hybrids more difficult due to the steric effect, thus leading to the slow growth rate and stable fluorescence of CdS grains inside. Fig. 3c and d corresponds to the detailed evolution process of the PL peaks of the control sample and CdS-latex hybrids over two months. It can be seen that the control sample undergoes a larger amount of redshift (over 50 nm) while the PL spectrum of the as-obtained CdS-latex hybrids nearly stay constant (less than 5 nm). The results further reveal that the adoption of the microreactor here offers more stable fluorescent materials bearing a narrower spectrum.

The obtained CdS-latex hybrids not only have stable fluorescence, but also are highly monodisperse, and thus can be assembled to large-scale fluorescent CPCs. Fig. 4 presents the optical photographs of CPC films constructed by the PS seed microspheres, the G2Vi-PS microspheres and the CdS-latex hybrids, respectively. It can be seen that the CPC film assembled by PS seed microspheres displays blue structural colour, while it changes to green after grafting copolymerization with the G2-Vi dendrimers due to the increase of particle size. The grafting process here do not impose negative effect on the assembly of resulting microspheres, giving the microreactor possibility to construct various functional CPCs. Fig. 4c shows the CPC film constructed by the as-obtained CdS-latex hybrids. It also displays bright yellowish green colour. It implies the method here takes obvious advantage over traditional methods that the G2Vi-PS microspheres retains regular morphologies and high monodispersity throughout the process. whereas, in the traditional approaches such as LbL technique or surface grafting method, the assembly of composite spheres are generally impeded because of surface defects or peculiar shapes.

The reflection spectrum of CPC films constructed by the PS seed microspheres, the G2Vi-PS seed microspheres and the CdS-latex hybrids are presented in Fig. 4d, respectively. For the CPC array of PS microspheres, a diffraction peak is noted at 481 nm, while that of the G2Vi-PS microspheres is 532 nm. For the CPCs, the relationship among the bandgap position, λ , the effective

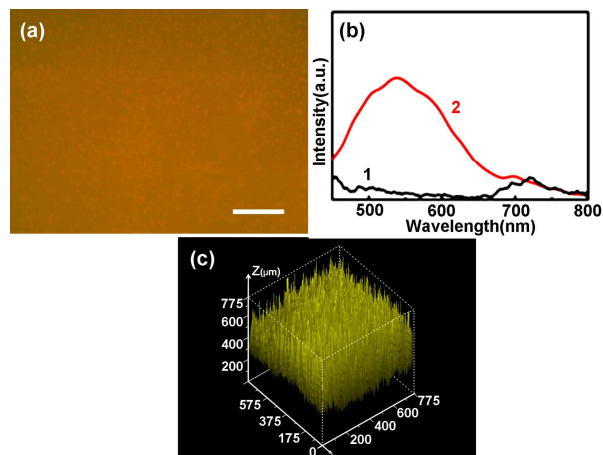


Fig. 5 (a) Fluorescence microscopy image of the CPC film constructed by the CdS-latex hybrids (Scale bar: 200 μm). (b) PL spectra of the films constructed by CdS-latex hybrids (Curve 1) and G2Vi-PS microspheres (Curve 2). (c) Distribution of PL intensity of the CPC film constructed by CdS-latex hybrids.

refractive index, n_{eff} , and the diameter of the building blocks is determined by $\lambda = 1.632n_{\text{eff}}D$. As the PS seed microspheres and G2Vi-PS microspheres have similar lattice constant, the redshift of the diffraction peak at this step is mainly caused by the size growth. After *in situ* generation CdS NCs, the diffraction peak for CdS-latex hybrids further shifts to 548 nm. Since the size of the CdS-latex hybrids is almost unchanged in comparison with that of G2Vi-PS microspheres (Fig. 1b and 2c), the redshift of the CPC array can be attributed to the increase of effective refractive index originated from doped CdS NCs. A 3% increase in effective refractive index was estimated for the CdS-latex hybrids, compared with the array assembled by G2Vi-PS microspheres. Moreover, the effective refractive indices of the G2Vi-PS microspheres and the CdS-latex hybrids were determined to be 1.44 and 1.48, respectively. As excess precursor metal ions were added to synthesize CdS NCs within G2Vi-PS microspheres, accordingly, the maximum NCs uptake capability for the microreactors can be estimated from n_{eff} of their self-assembled CPCs. We assume the volume fraction of the G2Vi-PS microspheres equals to 0.74, and use the relationship $n_{\text{eff}}^2 = 0.26n_a^2 + n_1^2(0.74-f) + n_2^2f$, where n_a , n_1 , and n_2 are the refractive indices of air, the G2Vi-PS microspheres and the CdS-latex hybrids, respectively, and f is the volume fraction of CdS in the CPC. For $n_1 = 1.56$ and $n_2 = 2.5$, f was estimated to be 0.034 and the CdS/polymer volume ratio in the microspheres was 4.9 vol.%.

The fluorescence properties of CPC films were further investigated. Fig. 5a shows the fluorescence microscopy image of the CPC film assembled by the CdS-latex hybrids. The film with bright structural colour also displays yellow fluorescence under UV light. As shown in Fig. 5b, its corresponding PL spectrum features a broad peak in the range of 440-660 nm originated from the *in situ* generated CdS NCs. Besides, a weak peak in the range of 660-790 nm is also detected owing to the polymer fluorescence of G2Vi-PS microspheres. In addition, the distribution of PL intensity of the as-obtained CPC film was investigated by the laser scanning confocal microscope. Fig. 5c shows the scans of a small area of the composite CPC films. The PL intensity at different locations is almost the same, indicating a highly uniform fluorescence of the as-obtained CPC films.

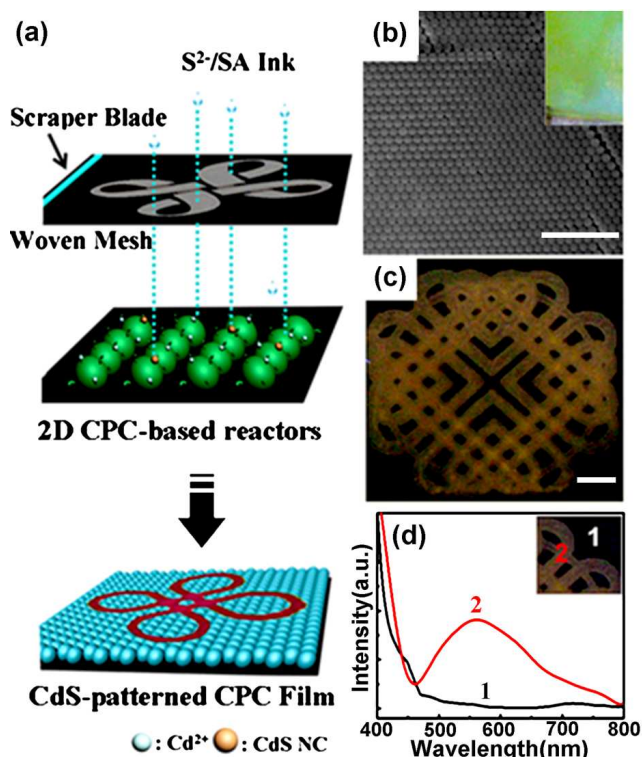


Fig. 6 (a) Schematic illustration of the process for preparation of CdS-patterned CPC films from 2D microreactor via silk screen printing. (b) SEM image of the 2D CPC film constructed by Cd²⁺-doped G2-Vi microspheres. (Scale bar: 2 μm). Inset: the corresponding microscopy image of the CPC film. (c) the fluorescence microscopy image of CdS-patterned CPC film. (Scale bar: 3 mm) (d) Fluorescence emission spectra ($\lambda_{\text{ex}} = 395 \text{ nm}$) of uncontact domains (1, black) and contact domains (2, orange). Inset: the corresponding fluorescence images.

From the results demonstrated above, we can see that the G2Vi-PS microspheres, bearing abundant thioether anchor sites can efficiently capture guest metallic components, can be used as 0D reactor for *in situ* generation of high uptake of NCs with controllable size. The as-obtained hybrids retain regular morphologies and high monodispersity throughout the process. Consequently, the CdS-latex hybrids can further self-assembled into large-scale ordered colloidal arrays, providing high-quality CPCs with uniform fluorescence.

Additionally, we explored the synthesis of NCs inside the 2D confined space of CPCs, which is meaningful for encoding, anti-counterfeiting or a set of relevant applications. To this end, a silk screen printing process was conducted, wherein a CPC film assembled by Cd²⁺-loaded G2-Vi microspheres was firstly prepared via a vertical deposition method, and the aqueous solution of the mixture of Na₂S and SA was used as the printing “ink”. The introduction of SA here greatly increases the viscosity of the printing ink. Thus, the lateral diffusion beyond the stencil was restrained, which is beneficial to high-quality silk-screen patterns.⁴⁹ As depicted in Fig. 6a, the ink was quickly casted onto the printing mask and penetrated through the mesh with a “Chinese Knot” pattern (160 meshes) onto the as-obtained CPC film underneath. After the evaporation of water at room temperature, the area contacted with the printing “ink” show strong fluorescence while the uncontacted region show no fluorescence peak in the visible range, through which the

fluorescent pattern was formed. As shown in Fig. 6b, the CPC film is long range order composed of uniform hexagonal-type close packed microspheres, and hence the CdS-patterned CPC film shows bright green structural color under daylight. Whereas, a orange fluorescence pattern of Chinese knotting finally comes out under UV light (Fig. 6c). Therefore, the CPC film shows bifunctional optical performance that it displays bright green structural color (inset of Fig. 6b) and orange-emitting “Chinese Knot” fluorescent pattern under UV light (Fig. 6d). Fig. 6d corresponds to the fluorescence emission spectra. No fluorescence was observed for the uncontact region of the CPC film, while a strong PL peak centered at 550 nm was detected for the contact region. It implies that the printing ink containing Cd²⁺ ions can react with the CPC substrate to form CdS NCs inside the 2D confined space, thus displaying reaction-induce-response fluorescence. The results suggest that by using a screen stencil oriented printing technique, bifunctional CPC films with on-demand fluorescent patterns can be freely and quickly constructed. More significantly, this process is suitable for other metal ions that can be extracted into the interior of dendrimers, providing a promising pathway to construct NC-integrated CPCs selectively and effectively.

Conclusions

The utilization of well-defined dendrimers to construct 0D and 2D reactors is demonstrated herein to facilitate the fabrication of CPCs with high-uptake NCs. As an independent 0D microreactor, G2Vi-PS microspheres bearing abundant thioether anchor sites can capture guest metallic components, followed by the introduction of chalcogenides, to realize *in situ* generation of higher-uptake NCs. Moreover, the resulting NC-latex hybrids can be directly self-assembled into large-scale ordered colloidal arrays, providing high-quality CPCs with uniform fluorescence. Additionally, compact assemblies of the Cd²⁺-loaded G2-Vi microspheres were prepared and employed as a large-scale 2D reactor for synthesis of NCs. By using a screen stencil oriented printing method, an on-demand fluorescent pattern is freely and quickly achieved via a reaction-induce-response process, constituting an alternative way to construct NC-integrated CPCs selectively and effectively. We believe the fundamental knowledge gained from the study of these 0D and 2D NC microreactors will facilitate progress in the field of self-assembled functional colloids and photonic materials.

Acknowledgements

This work was supported by the National High Technology Research and Development Program of China (863 Program) (2012AA030313), National Natural Science Foundation of China (21076103, 21176122 and 21006046), Specialized Research Fund for the Doctoral Program of Higher Education of China (20103221110001), Industrial Project in the Science and Technology Pillar Program of Jiangsu Province (BE2012181), and Priority Academic Program Development of Jiangsu Higher Education Institutions (PAPD).

Notes and references

- E. Yablonovitch, T. J. Gmitter and K. M. Leung, *Phys. Rev. Lett.*, 1991, **67**, 2295.
- S. John and J. Wang, *Phys. Rev. B: Condens. Matter*, 1991, **43**, 12772.
- D. J. Norris, E. G. Arlinghaus, L. Meng, R. Heiny and L. E. Scriven, *Adv. Mater.*, 2004, **16**, 1393.
- S. Kubo, Z. Z. Gu, K. Takahashi, Y. Ohko, O. Sato and A. Fujishima, *J. Am. Chem. Soc.*, 2002, **124**, 10950.
- J. Ge, Y. Yin, *Angew. Chem. Int. Ed.*, 2011, **50**, 1492.
- J. Wang, Y. Zhang, S. Wang, Y. Song and L. Jiang, *Acc. Chem. Res.*, 2011, **44**, 405.
- D. V. Skryabin, F. Luan, J. C. Knight and P. S. J. Russell, *Science*, 2003, **301**, 1705.
- M. Xu, A. V. Goponenko and S. A. Asher, *J. Am. Chem. Soc.*, 2008, **130**, 3113.
- S. H. Kim, S. J. Jeon, G. R. Yi, C. J. Heo, J. H. Choi and S. M. Yang, *Adv. Mater.*, 2008, **20**, 1649.
- Z. Yu, L. Chen and S. Chen, *J. Mater. Chem.*, 2010, **20**, 6182.
- K. Sumioka, H. Kayashima and T. Tsutsui, *Adv. Mater.*, 2002, **14**, 1284.
- Z. Nie, W. Li, M. Seo, S. Xu and E. Kumacheva, *J. Am. Chem. Soc.*, 2006, **128**, 9408.
- Z. Yu, C. F. Wang, L. Ling, L. Chen and Su Chen, *Angew. Chem. Int. Ed.*, 2012, **51**, 2375.
- W. Hong, X. Hu, B. Zhao, F. Zhang and D. Zhang, *Adv. Mater.*, 2010, **22**, 5043.
- A. D. Dinsmore, M. F. Hsu, M. G. Nikolaides, M. Marquez, A. R. Bausch and D. A. Weitz, *Science*, 2002, **298**, 1006.
- L. Hu, Z. Chena and M. J. Serpe, *Soft Matter*, 2012, **8**, 10095.
- Y. Li, E. C. Y. Liu, N. Pickett, P. J. Skabara, S. S. Cummins, S. Ryley, A. J. Sutherland, P. O'Brien, *J. Mater. Chem.*, 2005, **15**, 1238.
- X. H. Gao, S. M. Nie, *J. Phys. Chem. B.*, 2003, **107**, 11575.
- X.Y. Liu, Z.W. Niu, H.F. Xu, M.L. Guo, Z.Z. Yang, *Macromol Rapid Commun*, 2005, **26**, 1002.
- J. Riegler, O. Ehlert, T. Nann, *Anal. Bioanal. Chem.*, 2006, **384**, 645.
- C. Y. Jiang, S. Markutsya, Y. Pikus and V. V. Tsukruk, *Nat. Mater.*, 2004, **3**, 721.
- J. Li, X. W. Zhao, Y. J. Zhao, J. Hu, M. Xua and Z. Z. Gu, *J. Mater. Chem.*, 2009, **19**, 6492.
- C. N. Allen, N. Lequeux, C. Chassenieux, G. Tessier and B. Dubertret, *Adv. Mater.*, 2007, **19**, 4420.
- K. Ariga, J. P. Hilla and Q. Ji, *Phys. Chem. Chem. Phys.*, 2007, **9**, 2319.
- M. Antonietti, F. Grohn, J. Hartmann and L. Bronstein, *Angew. Chem. Int. Ed.*, 1997, **36**, 2080.
- M. Zhao, L. Sun, and R. M. Crooks, *J. Am. Chem. Soc.*, 1998, **120**, 4877.
- J. Zhang, N. Coombs, E. Kumacheva, Y. Lin and E. H. Sargent, *Adv. Mater.*, 2002, **14**, 1756.
- H. P. M. De Hoog, I. W. C. E. Arends, A. E. Rowan, J. J. L. M. Cornelissen and R. J. M. Nolte, *Nanoscale*, 2010, **2**, 709.
- S. Butuna and N. Sahiner, *Polymer*, 2011, **52**, 4834.
- M. Agrawal, A. Pich, S. Gupta, N. E. Zafeiropoulos, J. R. Retama and M. Stamm, *J. Mater. Chem.*, 2008, **18**, 2581.
- K. Akamatsu, M. Shimada, T. Tsuruoka, H. Nawafune, S. Fujii and Y. Nakamura, *Langmuir*, 2010, **26**, 1254.
- V. Kozlovskaya, E. Kharlampieva, S. Chang, R. Muhlbaier and V. V. Tsukruk, *Chem. Mater.*, 2009, **21**, 2159.
- S. Wang, D. G. Choi and S. M. Yang, *Adv. Mater.*, 2002, **14**, 1311.
- Y. K. Ee, R. A. Arif, N. Tansu, *Appl. Phys. Lett.*, 2007, **91**, 221107.
- P. Kumnorkaew, Y. K. Ee, N. Tansu, J. F. Gilchrist, *Langmuir*, 2008, **24**, 12151.
- P. Zhu, G. Liu, J. Zhang, N. Tansu, *J. Display Technology*, 2013, **9**, 317.
- X. H. Li, P. Zhu, G. Liu, J. Zhang, R. Song, Y. K. Ee, P. Kumnorkaew, J. F. Gilchrist, N. Tansu, *J. Display Technology*, 2013, **9**, 324.
- X. H. Li, R. Song, Y. K. Ee, P. Kumnorkaew, J. F. Gilchrist, N. Tansu, *IEEE Photonics Journal*, 2011, **3**, 489.

- 39 W. H. Koo , W. Youn , P. Zhu , X. H. Li , N. Tansu , F. So, *Adv. Funct. Mater.*, 2012, **22**, 3454.
- 40 C. Rissing and D. Y. Son, *Organometallics*, 2009, **28**, 3167.
- 41 L. Hou, L. Chen, and S. Chen, *Langmuir*, 2009, **25**, 2869.
- 5 42 L. Hou, C. Wang, L. Chen and S. Chen, *J. Mater. Chem.*, 2010, **20**, 1.
- 43 Q. Yan, Z. Zhou and X. S. Zhao, *Langmuir*, 2005, **21**, 3158.
- 44 L. Yan, Z. Y. Yu, L. Chen, C. F. Wang, and S. Chen, *Langmuir*, 2010, **26**, 10657.
- 45 C. Rissing and D. Y. Son, *Organometallics*, 2008, **27**, 5394.
- 10 46 C. Rim, L. J. Lahey, V. G. Patel, H. Zhang and D. Y. Son, *Tetrahedron Lett.*, 2009, **50**, 745.
- 47 L. Chen, T. E. Andersson, C. Rissing, S. Yang, S. Chen and D. Y. Son, *J. Mater. Chem. B*, 2013, **1**, 116.
- 48 M. Y. Gao, S. Kirstein and H. Möhwald, *J. Phys. Chem. B*, 1998, **102**, 8360.
- 15 49 J Wang, C. F. Wang, S Chen, *Angew. Chem. Int. Ed.*, 2012, **51**, 2375.